

Microwave holography in detection of hidden objects under the surface and beneath clothes

Andrey Zhuravlev¹, Alexander Bugaev², Sergey Ivashov¹, Vladimir Razevig¹, and Igor Vasiliev¹

¹Bauman Moscow State Technical University, Remote Sensing Laboratory, 5, 2nd Baumanskaya str., 105005 Moscow, Russia, azhuravlev@rslab.ru, sivashov@rslab.ru, vrazevig@rslab.ru, ivasiliev@rslab.ru

²Moscow Institute of Physics and Technology, Institutskii per., 9, 141700, Dolgoprudny, Moscow Region, Russia, bugaev@cplire.ru

Abstract

Proposed in the article design of a continuous wave radar with programmable frequency switching and quadrature receiver is targeted as base component to a variety of radars: ground penetrating radar, body scanner, and bio-radar. Algorithms of reconstructing holograms are outlined for planar and circular apertures. High achievable resolution is demonstrated in experiments involving measurements and reconstruction of holograms in air and opaque media.

1. Introduction

As an example of successful use of microwave holography it is possible to mention holographic subsurface radar RASCAN [1, 2]. The name holographic was given to this type of radar as it uses the same principle as it used in optical holography. There are two waves that influence the output signal: object wave that was reflected by a buried object and another due to receive-transmit antenna coupling and reflection from the surface. This interference pattern registered over sufficiently extent area of interest reveals highly detailed picture of what is beneath the ground. The radar is very sensitive to buried object depth variation though does not give absolute depth information. Post processing of images is usually not required due to attenuation and antenna directivity pattern. A fragment of a buried object is only visible when it is in close proximity to the antenna. The resulting hologram of a shallowly buried object resemble shadow silhouette of the object as diffraction effects are still weak at small distances and attenuation and near field sensitivity of the antenna result in almost no interference rings away from nadir. As the depth of a buried object increases, diffraction effects deteriorate the picture, making it look like interference pattern with distinctive interference stripes. In such a situation reconstruction algorithms are required. And even if reconstruction is usually not required in subsurface applications at shallow depths, it is necessary when the problem of detecting hidden objects under clothes emerges or the distance to a buried object increases. The rest of the article is organized as follows. The next section covers principal schematic of the radar. In Section 3 a reconstruction algorithm is outlined for the plane aperture with experimental examples. Circular aperture is considered in Section 4. Several application areas suggested in Conclusion.

2. System Design

The schematic of the radar is presented in Fig. 1. The design of the radar is based on available IC components: phase-locked loop frequency synthesizers and voltage-controlled oscillators (VCO). Depending on desired frequency range different VCO and synthesizers are available. In this project three radars sharing the same principle schematic were designed and assembled in the following frequency ranges: 3.6 – 4.0, 5.8 – 6.8, and 14 – 15 GHz. The reference frequency for the synthesizer is drawn from a 20 MHz crystal oscillator. Charge pump tuning pulses (CP output) are filtered, amplified, and fed into VCO. One output of VCO feeds transmit antenna and local oscillator input of the frequency mixer while other provides divided by 8 (for 15 GHz radar) feedback frequency. The signal from the receive antenna is mixed with in-phase and shifted by 90° components of the local oscillator, giving I and Q components of the received signal (direct conversion receiver). I and Q components are sampled by an ADC at programmable intervals. The microcontroller unit (MCU) uses SPI bus to initialize and control the synthesizer and ADC. Switching between frequencies is accomplished by programming internal registers of the

synthesizer via SPI bus. MCU is connected to a PC via USB. PC-side software allows acquiring, displaying, and storing data.

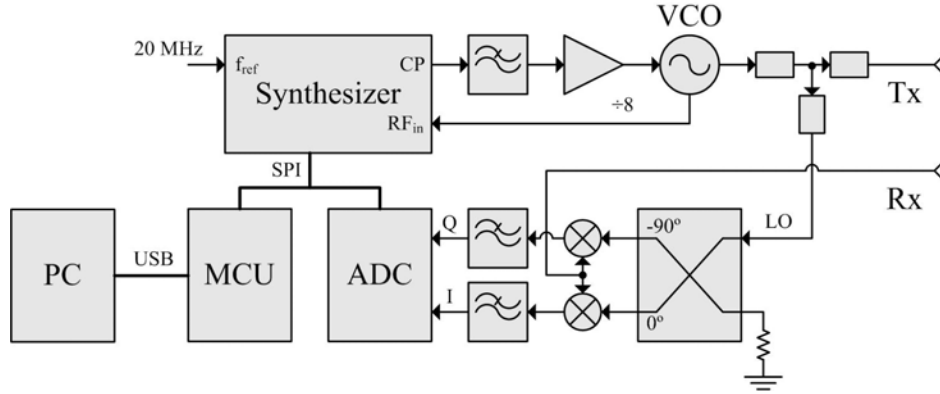


Fig. 1. Design schematic of the radar.

The assembled transmitter and receiver modules mounted on the antenna are shown in Fig. 2. The visible in the figure cables connect the assembly with MCU control unit. The maximal emitting power of the transmitter is limited by VCO and not greater than 7 dBm.

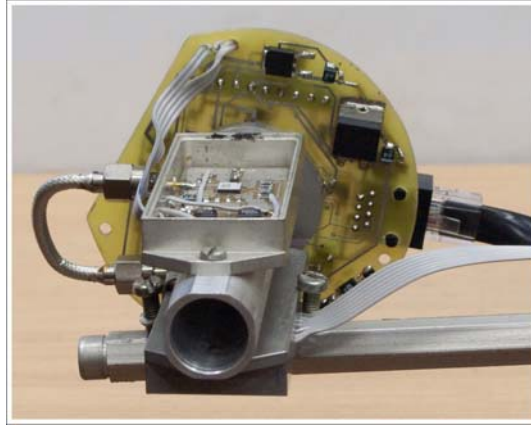


Fig. 2. Transmitter and receiver modules for 14-15 GHz frequency range mounted on the antenna.

3. Holograms over planar aperture

Two types of most common apertures were considered to register and reconstruct holograms: planar and circular. The reconstruction algorithm for a planar aperture is based on Fourier decomposition of registered complex amplitude of the signal [3]. The key relationships can be summarized as follows:

$$\hat{E}(u_1, u_2; 0) = \frac{1}{(2\pi)^2} \int_{-\infty}^{\infty} \int_{-\infty}^{\infty} E^*(x, y) \exp[-i(u_1 x + u_2 y)] dx dy \quad (1)$$

$$\hat{E}(u_1, u_2; z) = \hat{E}(u_1, u_2; 0) \exp\left[-i\sqrt{(2k)^2 - u_1^2 - u_2^2} z\right] \quad (2)$$

$$E_R(x, y, z) = \int_{-\infty}^{\infty} \int_{-\infty}^{\infty} \hat{E}(u_1, u_2; z) \exp[i(u_1 x + u_2 y)] du_1 du_2 \quad (3)$$

In equation (1) plane-wave spectrum of registered complex amplitude distribution in plane XOY ($z=0$) is obtained by two-dimensional Fourier transform of complex conjugate of the complex amplitude. Equation (2) relates plane-wave spectra at parallel planes separated by z . The doubled wave number is explained by the fact that the

receiver and transmitter are in the same position. Equation (3) gives reconstructed distribution of sources by inverse Fourier transform of plane-wave spectrum at z .

An example of microwave hologram (in-phase component) by two intersecting metallic rulers placed under a stack of dry plaster sheets at the depth of 14.7 cm is shown in Fig.3 on the left. The sizes of rulers are 32 by 2 and 32 by 5 cm. The hologram was registered at 3.75 GHz. It can be seen in the figure that the interference pattern does not convey actual sizes of the objects while the reconstructed image does. It is easily seen that actual sizes of the rulers differ.

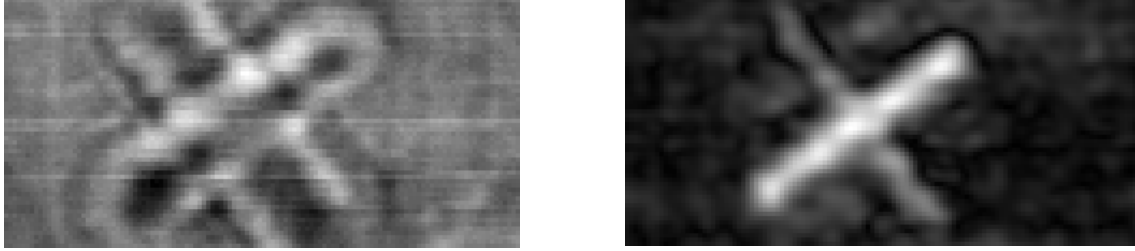


Fig. 3. Microwave hologram of two metallic rulers under the stack of plaster sheets at the depth of 14.7 cm (left). Reconstructed image (right). Sounding frequency – 3.75 GHz.

The requirement to reconstruct holograms of buried objects emerges when their depth exceeds an order of several wavelengths. The interference pattern produced by shallowly buried objects or at close range may not have interference stripes as diffraction effects are still weak.

4. Holograms over circular aperture

In the problem of detecting hidden objects under clothes a cylindrical aperture is usually used. Scanning over a cylindrical aperture has some advantages over plane apertures for this particular task as the distance to the sensor stays minimal during a body scan and each side of the body is illuminated.

When processing holograms registered over a cylindrical aperture application of fast Fourier transform algorithms is not straightforward as it was for plane holograms. A common approach usually involves signal interpolation over an equidistant rectangular spatial grid or application of non-uniform Fourier transform [4, 5].

The reconstruction procedure that was used in this work is based on [6] and summarized by equations (4) and (5). In relationship (4), $E(i,j)$ represents samples of complex amplitude. Index i changes when moving along a circle in horizontal plane while j changes when moving vertically.

$$I(\mathbf{r}_f) = \left| \sum_{i,j} E(i,j)E(i,j;\mathbf{r}_f)W(i,j;\mathbf{r}_f) \right| \quad (4)$$

In equation (4) $E(i,j;\mathbf{r}_f)$ is the focusing operator given by the following expression:

$$E(i,j;\mathbf{r}_f) \equiv E(\mathbf{r}_{i,j};\mathbf{r}_f) = \frac{\exp(-i2k|\mathbf{r}_{i,j}-\mathbf{r}_f|)}{|\mathbf{r}_{i,j}-\mathbf{r}_f|^2}, \text{ where } i=1,2,\dots,M; \quad j=1,2,\dots,N. \quad (5)$$

$W(i,j;\mathbf{r}_f)$ is a window function. The support of this function depends on the focusing point position and calculated adaptively to take into calculations the area of hologram that is most responsible for reconstruction for a given focusing point [7]. The result of the reconstruction procedure $I(\mathbf{r}_f)$ in equation (4) gives distribution of virtual sources creating the hologram.

An example of applying the described reconstruction procedure to a sample hologram recorded at 13.6 GHz is shown in Fig. 4. The exposed object was a short fragment of plastic cylinder shifted from the center of the cylindrical aperture by 2.5 cm. The radius of the aperture was 6 cm.

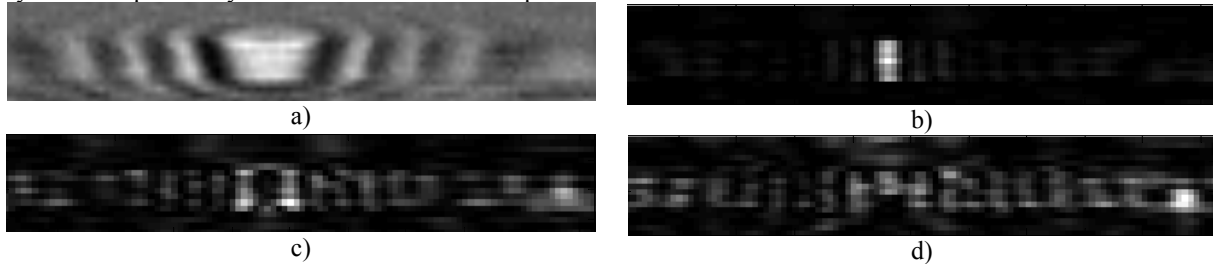


Fig. 4. Cylindrical hologram of an off-center plastic cylinder and its reconstruction: a) in-phase component of the hologram, b) focusing at the concentric cylinder with radius 2.2 cm, c) focusing at 2.5 cm, d) 3 cm.

5. Conclusion

The suggested design of a continuous wave radar with programmable frequency switching and quadrature receiver is based on mass market integral circuits what can make ultimate devices cheap and available. Designs of ground penetrating radar, body scanner, and bio-radar [8] can share the considered schematic. The experimental results demonstrate high achievable resolution in subsurface sounding. The resolution is comparable to millimeter-wave body scanners.

6. Acknowledgement

This work was supported by Russian Foundation for Basic Research, International Science and Technology Center (Project #2541), and grant of the President of the Russian Federation MK-118.2011.9.

7. References

1. V.V. Razevig, S.I. Ivashov, I.A. Vasiliev, A.V. Zhuravlev, T. Bechtel, L. Capineri, P. Falorni, "RASCAN Holographic Radars as Means for Non-Destructive Testing of Buildings and Edifical Structures," *Proceedings of the Structural Faults and Repair-2010*, June 15 – 17, 2010, Edinburgh, Scotland, UK.
2. S. Ivashov, V. Razevig, I. Vasilyev, A. Zhuravlev, T. Bechtel, L. Capineri, "The Holographic Principle in Subsurface Radar Technology," *International Symposium to Commemorate the 60th Anniversary of the Invention of Holography*, Springfield, Massachusetts USA, October 27-29, 2008, pp. 183-197.
3. Sheen D.M., McMakin D.L., Hall T.E., "Three-dimensional millimeter-wave imaging for concealed weapon detection," *Microwave Theory and Techniques, IEEE Transactions on*, vol.49, no.9, pp. 1581-1592, Sep 2001.
4. A. Dallinger, S. Schelkshorn, and J. Detlefsen, "Efficient ω -k-algorithm for circular SAR and cylindrical reconstruction areas," *Adv. Radio Sci.*, 4, 2006, pp. 85-91.
5. B. Subiza, E. Gimeno-Nieves, J.M. Lopez-Sanchez, and J. Fortuny-Guasch, "Non-uniform FFT's (NUFFT) algorithms applied to SAR imaging," *SAR Image Analysis, Modeling, and Techniques VI, Proceedings of SPIE Vol. 5236*, Bellingham, WA, 2004.
6. Y.J. Kim, L. Jofre, F. De Flaviis, M.Q. Feng, "Three-dimensional microwave imaging technology for damage detection of concrete structures," *Proc. SPIE 5057*, 29, 2003.
7. Feinberg E.L., *Propagation of radiowaves along the terrestrial surface*, Nauka-Fizmatlit, 1999, 496 p. (in Russian).
8. A.S. Bugaev, I.A. Vasil'ev, S.I. Ivashov, and V.V. Chapurskii, "Methods of Detection of Human Breathing and Heartbeat," *Journal of Communications Technology and Electronics*, 2006, Vol. 51, No. 10, pp. 1154–1168.